macla nº 19. julio '14
revista de la sociedad española de mineralogía

Combined multianalytical approach for the characterization of commercial bricks with a view to their technical use

/ CHIARA COLETTI* (1) / GIUSEPPE CULTRONE (2) / LARA MARITAN (1) / CLAUDIO MAZZOLI (1)

(1) Department of Geoscience, University of Padova, Via G. Gradenigo 6, 35131, Padova (Italy)
(2) Department of Mineralogy and Petrology, University of Granada, Avda. Fuentenueva, s/n 18002, Granada (Spain)

INTRODUCTION

Brick is a construction material used in buildings since Roman times and still used in modern constructions for its own technical features and aesthetic qualities. The raw materials and the firing temperatures are closely related with the characteristics of fired products *(Riccardi et al., 2009)*.

During the firing process mineralogical and textural transformations occur (and resembles the high-temperature metamorphism) which produces an artificial material characterized by a significant porosity. Porosity is an important parameter to evaluate the durability of bricks, especially in aggressive environments, e.g. those in which salts and frost are present (*Cultrone et al., 2004*).

This work aims to develop a combined multianalytical approach for studying the relationships between mineralogical-textural and physical-mechanical characteristics and decay behavior of five types of industrial bricks. They have been chosen in order to define the influence of raw materials and firing temperatures in the development of different mineralogy, micro-texture and porosity.

MATERIALS AND METHODS

Five industrial bricks (GP, N, R6, RSS and RS) produced in north-east Italy using local available clays have been characterized. GP and N were fired at 1050°C, RS at 980 ºC, RSS at 950 ºC and R6 at 600°C.

Bulk chemical characterization was carried out through X-ray fluorescence analysis (XRF), while mineral assemblages were defined by X-ray powder diffraction (XRPD). Mineralogical and textural features were analyzed by combining optical and electronic microscopy, this last by means of a Field Emission Scanning Electron Microscopy (FESEM) equipped with EDX microanalysis.

Pore size distribution was determined using mercury intrusion porosimetry (MIP). The study of the pore system was completed measuring water absorption and drying (hydric tests) of samples. Finally, the durability of brick was evaluated by means accelerated ageing tests (freeze-thaw and salt crystallization tests), and monitored by means of ultrasounds.

RESULTS AND DISCUSSION

Mineralogy and texture

Macroscopically, RSS, RS and R6 are red-coloured, while GP and N are, respectively, yellow and dark grey.

Under the optical microscope, samples are texturally homogeneous and show a porosity comprised between 20 and 40%. Pores are generally small to medium in size with vesicles and vughs (rarely channels) shapes. The modal analysis of inclusions shows a grain-size distribution moderately selected for R6 and RSS and not selected for GP, N and RS. The volume of inclusions with respect to the groundmass is 40% for RSS, RS and R6 and 10-20% for GP and N.
Table 1 shows the chemical composition of the five bricks. We can see that N and GP are the richest in CaO and MgO, while RSS and R6 are the richest in SiO_2. Finally, RS has intermediate CaO, MgO and SiO_2 contents.

XRPD analysis shows that RSS, RS, GP and N samples (fired over 900°C) are characterized by a similar mineralogy (quartz, wollastonite, gehlenite, plagioclase, K-feldspar and diopside). On the contrary, in R6 (fired at 600°C) phyllsilicates are still present and there are peaks of calcite and dolomite. This is because illite dehydroxylated at 700°C and carbonates decomposition occur between 650 and 900°C . Calcite reacts with quartz to form wollastonite and with illite to develop gehlenite *(Duminuco P. et al., 1998)*. Feldpars were detected in all samples. R6 contains feldspars proceeding from the raw material; in the other samples there are also the new-formed anorthite and sanidine. Moreover, at temperature range of 900-1050°C diopside is arranged from the reaction of dolomite with quartz. Sample N is rich in bustamite, $CaMn(Si_2O_6)$, developed from reaction of Mn-oxides (added to the raw material before firing) with calcite and quartz.

FESEM allowed to examine the processes of dehydroxylation and decarbonation in R6. Phyllosilicates maintain the sheet-like fabric, although, the lost of OH^- groups makes visible the exfoliation along their (001) planes *(Cultrone et al., 2005*). Carbonates are still recognizable, but with evident secondary porosity due to releasing of CO^2. In addition, it's evident the alteration of feldspar grains along exfoliation lines and the boundaries. The groundmass is still without melting.
In RS and RSS samples dehydroxylation of phyllosilicates is more extended and new Ca-silicates are developing at the rims of carbonates (fig 1).

GP and N samples show melted groundmass and reaction bridges, with marked boundaries in which new phases (gehlenite and diopside) have been developed, especially along quartz and

	SiO_2	Al_2O_3	Fe_2O_3	MnO	MgO	CaO	Na_2O	K_2O	TiO_2	P_2O_5
GP	50.17	13.19	4.80	0.09	5.61	20.39	0.72	2.84	0.49	0.13
N	42.41	11.67	4.93	12.86	4.93	17.63	0.60	2.66	0.52	0.15
RS	59.46	14.53	4.94	0.09	3.69	11.06	0.89	2.99	0.59	0.13
RSS	63.79	15.28	5.16	0.11	2.87	7.01	0.99	3.20	0.66	0.13
R6	60.32	14.35	4.85	0.11	2.69	6.22	0.93	3.03	0.64	0.13

Table 1. X-Ray fluorescence analysis of GP, N, RS, RSS and R6 samples.

palabras clave: ladrillo, mineralogía, porosidad, durabilidad | ***key words:*** brick, mineralogy, porosity, durability

* corresponding author: **chiara.coletti@studenti.unipd.it**

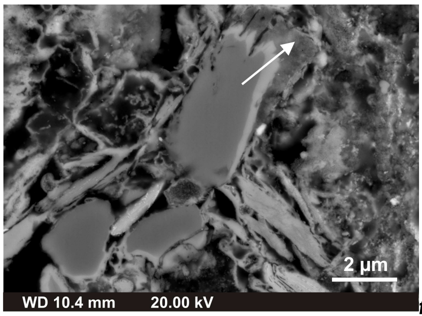

fig 1: BSE-FESEM image of RSS sample. Reaction along feldspar boundaries with Ca-enrichment and an intermediate passage to gehlenite (see arrow).

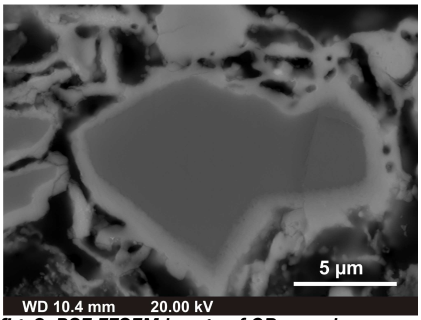

fig. 2: BSE-FESEM image of GP sample. Quartz grain with a reaction of diopside.

	A_b	A_f	A_x	*Di*	p_o	*Ks*	*ΔM*	*v*	*E*	*G*	*K*
GP	27.63	28.71	3.76	1.35	41	0.058	12.26	0.36	3.38	2.29	4.01
N	25.08	25.85	2.98	1.36	40	0.044	10.73	0.45	1.36	1.18	5.14
RS	22.60	23.09	2.12	1.36	37	0.039	14.26	0.35	2.53	1.70	2.72
RSS	21.57	23.28	7.35	1.37	37	0.044	18.07	0.34	1.55	1.04	1.71
R6	17.36	18.88	2.91	1.37	31	0.021	20.38	0.31	1.25	0.81	1.11

***Table 2.** Hydric parameters: A_b, free water absorption (%); A_f, forced water absorption (%); A_x, degree of pore interconnection (%); Di, drying index; p_o, open porosity (%), Ks, capillarity coefficient, (g/m^2 s$^{0.5}$). Ultrasounds:* ΔM, total anisotropy (%); v, Poisson's ratio, Young's modulus (MPa); G, shear modulus (MPa); K, bulk modulus (MPa).

feldspar grains (fig. 2). Secondary bubbles have developed in phyllosilicate pseudomorphs. Only in N bricks, bustamite is diffused in many grain boundaries.

Mineral phases in trace amounts, such as zircon and ilmenite, were detected in all samples.

Pore system

Hydric tests (Table 2) show that GP is the sample with the highest free and forced water absorption values (A_b and A_f). N, RS and RSS have intermediate indices, while R6 stands out for its low absorption. RS is characterized by a better pore interconnection (Ax) followed by R6 and N. RSS has the highest value which indicates the presence of pores with difficult access. All samples dry within 200 hours and show similar drying index (Di). Open porosity values (p_o) are linked to the carbonate content of samples. In fact, GP and N, the most carbonatic, have the highest values of open porosity, RSS and RS are intermediate and R6 is the lowest.

Results of capillarity test confirm the trend followed by free water absorption. GP is the most susceptible sample to capillarity rise (Ks), while R6 shows the lowest value. N, RS and RSS are in the middle. This factor suggests the presence of a pore system in GP bricks more sensible to deterioration compared to the other samples.

MIP analysis shows that all bricks have maximum radius close to 1 µm. More in detail, GP and N show a unimodal pore size distribution; RS and RSS have a bimodal trend; finally, R6 is characterized by pores with sizes comprised between 0.001 and 1 µm and larger pores with a size of 100 µm.

Compactness

The highest ultrasonic waves' velocities were measured in GP and N samples, while the lowest belong to R6. This suggests that GP and N are the most compact while R6 is the most porous sample. This last sample is also the brick with the highest anisotropy which can be explained by the presence of phyllosilicate sheets (*Cultrone et al., 2005*). With the increase of firing temperatures samples became texturally more homogeneous and anisotropy decreases (Table 2).

Poisson ratio (v) shows similar values for all samples, with a small rising in correspondence of those more carbonatic. GP stands out for the highest shear (G) and Young moduli (E). The others have similar results, with the lowest in R6. The highest compressive modulus (K) was found for N sample, followed by GP, while the other show lower results comprised between 1 and 3 MPa (Table 2).

Durability

Data from freeze-thaw test show a similar initial behavior for all samples. R6 is the less durable sample characterized by loss of fragments and development of fissures and cracks.

Salt crystallization test caused the development of damage in particular in correspondence of brick edges. R6 was again the weakest sample. The other samples showed a similar trend. Changes in the pore system after salt crystallization are confirmed by MIP analysis. All MIP curves are shifted in the pore range comprised between 20-100 µm.

CONCLUSIONS

The following conclusions can be drawn:
- although GP and N samples show greater mineralogical changes, they are the most susceptible to water absorption and capillarity rise.
- GP shows the best mechanical resistances.
- RS has the best pore interconnection, while RSS has the worst.
- R6 is the most exposed brick under accelerated decay tests.

The multianalytical approach adopted highlights the closed relationship among mineralogy, porosity, and physical properties and prove how these factors influence bricks behavior under different stress environments (presence of water, salt crystallization and freeze-thaw cycles).

ACKNOWLEDGEMENTS

This work is the result of collaboration between the brick company producer, San Marco s.r.l., and the Universities of Padua (Italy) and Granada (Spain).

REFERENCES

Cultrone G., Sebastián E., Elerta K., de la Torreb M. J., Cazalla O., Rodriguez–Navarro C. (2004): Influence of mineralogy and firing temperature on the porosity of bricks. Journal of the European Ceramic Society ***24****, 547–564*

—, —, Torreb M. J., (2005): Mineralogical and physical characterization of the bricks used in the construction of the "Triangular Bastion", Riga (Latvia). Applied Clay Science ***28****, 297–308*

Duminuco P., Messiga B., Riccardi M.P. (1998): Firing process of natural clays. Some microtextures and related phase composition. Thermochimica Acta ***321****, 185-190*

Riccardi M.P., Messiga B., Duminuco P. (2009): An approach to the dynamics of clay firing. Applied Clay Science 15, 393–409